*Progress In Electromagnetics Research M, Vol. 33, 95–104, 2013*

# A MONOLITHIC FREQUENCY SELECTIVE STRUCTURE WITH DUAL-BAND QUASI-ELLIPTIC FILTERING RESPONSE

**Xianjun Huang*, Peiguo Liu, Jianfeng Tan, Dongming Zhou, and Gaosheng Li**

College of Electronic Science and Engineering, National University of Defense Technology, Changsha 410073, China

**Abstract**—This paper presents the design of a monolithic structure with dual-band quasi-elliptic frequency selective filtering responses. The frequency selective structure consists of a two-dimensional (2-D) array of cavities apertured with six ring slots. The transmission response is with a quasi-elliptic passband in lower frequency, and an elliptic passband in upper frequency. By placing transmission zeros near the passband edge, the proposed structure is characterized with high selectivity, rapid rolloff, and high separation between two passbands. Besides, the working principles and influence of the dimensional parameters are fully investigated with simulations and analysis, which is helpful to the design. In this design, five resonances and three transmission zeros are obtained with a simple unit by introducing coupling and phase controlling. This work will be meaningful in study of three dimensional frequency selective structures with high performance.

## 1. INTRODUCTION

Three-dimensional (3-D) frequency selective structure (FSS) is a recent research topic [1, 2] and has attracted much interest because of some merits compared with traditional frequency selective surfaces [3–5]. In traditional planar layered frequency selective surfaces, the filtering responses meet the Butterworth or Chebyshev functions [6]. However, the elliptic response which is superior in high selectivity can hardly be accomplished in traditional designs for the absence of cross

*Received 5 August 2013, Accepted 10 October 2013, Scheduled 10 October 2013*

* Corresponding author: Xianjun Huang (huangxianjun001@163.com).

coupling [7, 8]. In 3-D FSSs, an outstanding point is the design of elliptic or quasi-elliptic filtering responses.

Recently, some 3-D FSSs with elliptic filtering response have been reported. A stable elliptic bandpass response under large incident angle was presented with 2-D periodic array of shielded microstrip lines [9]. Based on the concept of substrate integrated waveguide (SIW), Luo developed a series of 3-D FSSs with quasi-elliptic response, and realized an elliptic FSS with the method of cascading [8]. However, the elliptic FSS employing multi-layered structures is hard to tune for the redundancy of structural parameters, and is difficult to ensure precision of fabrication. Besides, by combining two kinds of FSS with one transmission zero separately, an elliptic FSS was published in [10].

Multi-band frequency selective surface has been comprehensively researched in traditional designs, while few works have been reported in multi-band quasi-elliptic or elliptic FSS. Luo commented the methods of multi-band frequency selective surface design, and contributed a FSS with two quasi-elliptic passbands using double square loop slots and an SIW cavity. The attenuation between two passbands increases fast for the presence of a transmission zero near the left edge [11]. If two transmission zeros are placed near both band edge, attenuation is believed to slump in a small frequency band, which is valuable in some applications requiring both close passband spacing and high stopband attenuation.

Besides, in traditional designs, one resonance frequency always corresponds to one resonance structure in unit, thus designing numbers of resonances and transmission zeros in multi-band quasi-elliptic FSSs will result in designing complexity. However, using the phase controlling and mutual coupling properly, a simple monolithic structure can exhibit multi-band quasi-elliptic responses with several resonances and transmission zeros.

In this paper, a dual-band FSS having a quasi-elliptic passband and an elliptic passband was designed with simple monolithic units. By placing three transmission zeros around the passband edge, a high separation between two passbands is achieved. This work can not only provide valuable reference in designing elliptic FSS, but also meet the demands of applications requiring both close passband spacing and high separation.

## 2. STRUCTURE MODEL AND RESPONSES

Figure 1 shows the geometry of the proposed FSS unit cell. As can be seen, a metallic cavity is apertured with six ring slots in each face, and filled with dielectric medium. Slots in opposite surfaces have

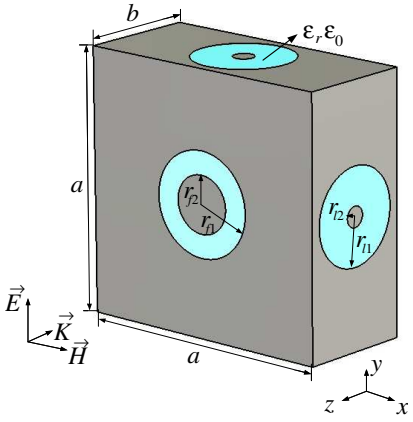


**Figure 1.** Geometrical configuration of FSS unit cell.

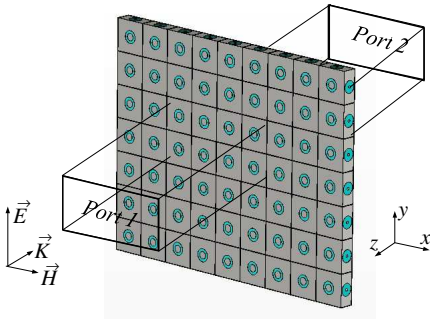


**Figure 2.** 2-D periodic array of unit structures and simulation configuration.

the same structural parameters, and the upper and lateral slots are symmetrical. The origin of coordinate (0, 0, 0) is placed at the center of the unit structure. In this paper, only the case of TE normal incidence is discussed ($E$-field is along $Y$-axis), considering that responses to vertically and horizontally polarized normal incidence are identical due to the geometrical symmetry.

As depicted in Figure 2, the FSS comprises a periodic array of unit structures in $x$- and $y$-directions. To get the filtering response, a TE normal incidence ($E$-field is along $Y$-axis, wave vector is along negative $z$-axis) is applied in Port 1.

From the simulated result in Figure 3, the FSS is with dual passbands. The lower passband centered at 8.98 GHz is formed with two resonances in reflection response, leading to a 3 dB bandwidth from 8.86 GHz to 9.11 GHz (250 MHz). In the transmission response, a transmission zero presents at 9.2 GHz, contributing to a slump of transmission loss from 3 dB to 57 dB when the frequency increases from 9.11 GHz to 9.2 GHz. The transition band is as low as 90 MHz. In a word, the lower passband is a typical quasi-elliptic response.

The upper passband exhibits an elliptic filtering response. As shown, three resonances at 11.82 GHz, 12.12 GHz and 12.33 GHz can be observed, which causes a 3 dB passband from 11.77 GHz to 12.34 GHz (570 MHz), and the maximum insertion loss in passband is 1.3 dB. An evident specialty in upper passband is that two transmission zeros are placed near the band edge, giving rise to a sharp rise of attenuation.

Near the left edge, attenuation soars from 3 dB at 11.77 GHz to 48 dB at 11.63 GHz, and hence the transition band is 140 MHz. Similarly, in the right edge, the transition band is only 30 MHz, resulting from the transmission zero at 12.37 GHz. In addition, with the appearance of two transmission zeros at 9.2 GHz and 11.63 GHz, the attenuation between two passbands is higher than 20 dB. As analyzed in the following Part III, these two transmission zeros are controlled by different structure parameters, which is quite helpful to accomplish a design with high passband separation and close passband spacing simultaneously. It should also be noticed that, similar with the elliptic circuit filter design, the abovementioned superior characters in the stopband are achieved in price of ripples in passband [12].

## 3. WORKING PRINCIPLES AND ANALYSIS

This part will focus on the operating principle of the proposed FSS and analyze effects of structural parameters. The discussion will be divided into two sections corresponding to dual bands. Besides, the following electrical field distribution figures are simulated under structural parameters in Figure 3.

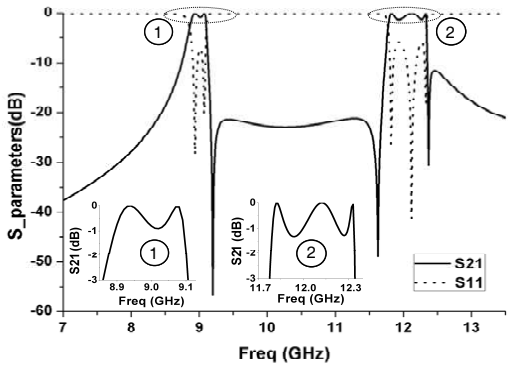


**Figure 3.** $S$-parameters of proposed FSS with parameters: $a = 23.6\,\text{mm}$, $b = 10.3\,\text{mm}$, $r_{f1} = 4.78\,\text{mm}$, $r_{f2} = 2.63\,\text{mm}$, $r_{l1} = 4.47\,\text{mm}$, $r_{l2} = 0.95\,\text{mm}$, $\varepsilon_r = 2.2$, and thickness of metal $t = 0.2\,\text{mm}$. Insets are the details of $S_{21}$ in corresponding areas.

### 3.1. Lower Passband

In Figure 3, the lower quasi-elliptic passband arises from two resonances. The first resonance at 8.94 GHz is produced by the slot resonance of the front ring. It occurs when the perimeter of the ring slot

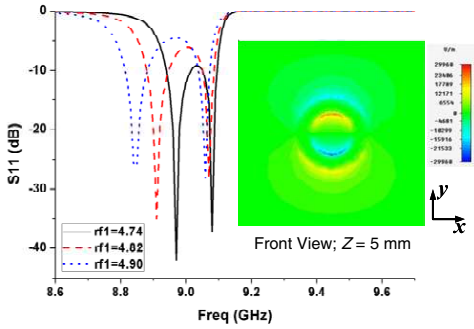


**Figure 4.** Reflection responses in lower frequency with varying $r_{f1}$. Insertion is the electrical field distribution at 8.94 GHz.

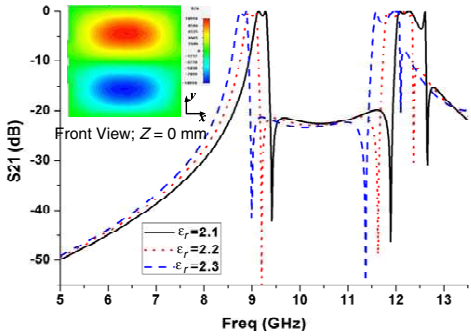


**Figure 5.** Transmission responses with different relative permittivity $\varepsilon_r$ and electrical field distribution at 9.08 GHz.

is a multiple of equivalent wavelength. Figure 4 gives detailed effect of parameter $r_{f1}$, and the inset is the electrical field distribution at 8.94 GHz. As illustrated, the electrical field mainly distributes near the slot. Moreover, with the increase of $r_{f1}$, the first resonance frequency becomes smaller accordingly, while the second resonance frequency keeps almost fixed.

The second resonance is the consequence of the cavity resonance. As revealed in the electrical field distribution in Figure 5, it derives from the TE120 mode of cavity resonance. With the cavity resonance theory, the resonance frequency can be roughly calculated with Equation (1) [13].

$$(f_r)_{mnp} = \frac{1}{2\sqrt{\varepsilon\mu}}\sqrt{\left(\frac{m}{a'}\right)^2 + \left(\frac{n}{b'}\right)^2 + \left(\frac{p}{c'}\right)^2}. \quad (1)$$

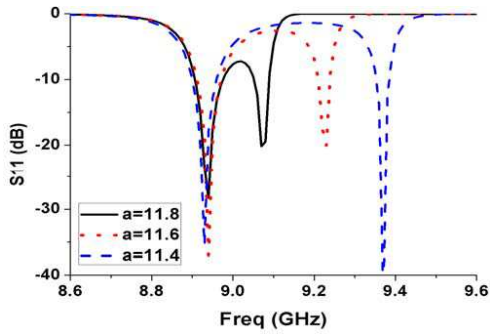


**Figure 6.** Reflection of FSSs with different parameter $a$.

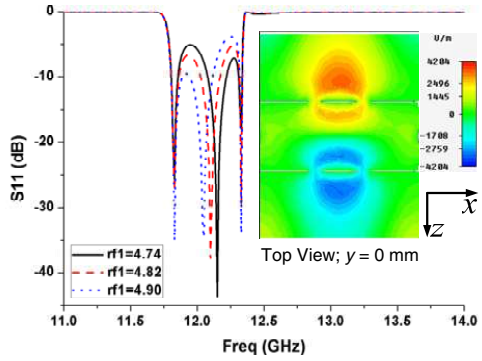


**Figure 7.** Reflections in upper passband with different parameter $r_{f1}$, and electrical field distribution at 12.12 GHz.

$$\varepsilon = \varepsilon_r \varepsilon_0. \tag{2}$$

When $a' = b'$ and $m = 1$, $n = 2$, $p = 0$,

$$(f_r)_{120} = \frac{1}{2\sqrt{\varepsilon_r \varepsilon_0 \mu_0}} \frac{\sqrt{m^2 + n^2}}{a'} = \frac{c_0}{a'} \frac{1}{2} \sqrt{\frac{5}{\varepsilon_r}} \tag{3}$$

where $C_0$ is the light speed in vacuum.

Since the cavity is apertured in each face, $a'$ is an equivalent dimension that is slightly bigger than $a$ [14].

Equation (3) suggests that, the bigger the parameters and $a$ and $\varepsilon_r$, the lower the second resonance frequency is. This can be verified by simulated curves in Figures 5 and 6. Additionally, Figure 5 indicates that using filling materials with high permittivity is a significant way to reduce the electrical dimension of the FSS.

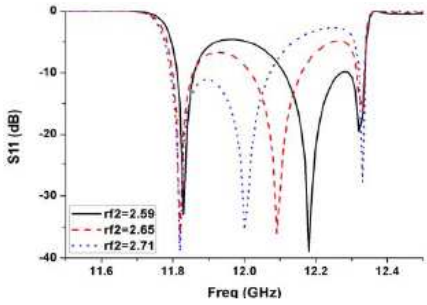


**Figure 8.** Reflection responses with different $r_{f2}$.

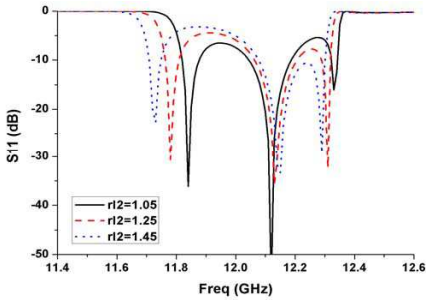


**Figure 9.** Reflection responses with different $r_{l2}$.

The transmission zero at 9.2 GHz is the result of mutual coupling of the ring slot resonance and TE120 cavity mode. Moreover, when the cavity resonance frequency is tuned to be smaller than the slot resonance frequency, the transmission zero will move to the left edge of the lower passband. It might be possible to get elliptic response in this band by adding another resonance nearby.

### 3.2. Upper Passband

The upper passband is a typical elliptic response with three resonances. The second resonance at 12.12 GHz originates from front ring resonance, and is mainly impacted by its parameters $r_{f1}$, $r_{f2}$. Figure 7 provides how the outer radius of the front ring $r_{f1}$ affects the reflection response in higher passband. As sketched, the second resonance frequency in upper passband ascends with the descent of $r_{f1}$, whereas $r_{f1}$ almost has no function on the first and the third resonances in this band. In addition, the inserted electrical field distribution demonstrates again that the front ring slot is the source of resonance at 12.12 GHz.

The following Figure 8 is another proof of the source of the second resonance. The effect of varying $r_{f2}$ resembles the case of $r_{f1}$. With the conclusion that the other two resonances in this passband keep almost fixed when $r_{f1}$, $r_{f2}$ shift in some range, it is easy to tune the ripples in the passband without changing the bandwidth.

The interpretation of the other two resonances in higher passband is relatively complicated, but is the soul of the elliptic FSS design using phase controlling and coupling.

Figure 9 elucidates the influences of parameter $r_{l2}$ of the lateral rings. Because the parameters $r_{l1}$ and $r_{l2}$ have the similar influences on

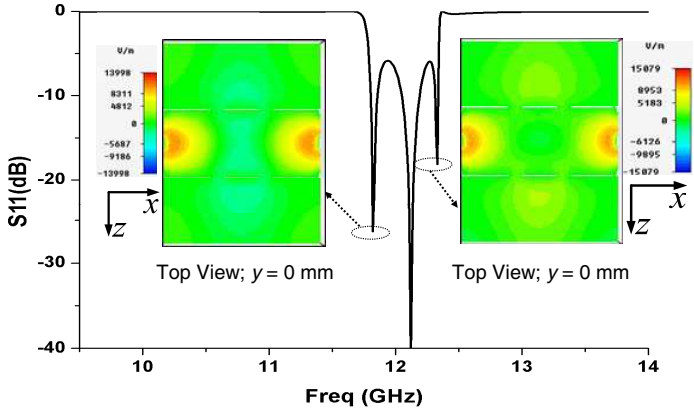


**Figure 10.** Electrical field distribution at 11.82 GHz and 12.33 GHz.

the reflection responses of the upper passband, only effect of parameter $r_{l2}$ is given here. From the figure, the frequencies of the first and the third resonances rise with the fall of parameter $r_{l2}$. However, the parameters of the lateral rings have little impact on the second resonance. Combined with the function of the front rings mentioned above, it can be summarized that the second resonance in upper passband is controlled by the parameters of front rings, while the first and the third ones are dominated by lateral rings. This separation is quite beneficial in tuning and poses much convenience in design.

However, from the field distribution of resonance frequencies shown in Figure 10, even though the lateral rings enjoy the domination of the first and third resonances, the resonance near the front rings also matters. By comparing the phase differences of electrical field in Figure 10, it is apparent that at 11.82 GHz, the fields near the front rings and the lateral rings are with the inversed phases, while fields at 12.33 GHz are in phase. Due to the comparative weakness of the field near front rings, the difference in phase makes the lateral rings produce two resonances, and they are closely placed in frequency.

The transmission zero is a typical symbol of elliptic responses. With analysis of the field distribution, it is not difficult to find that the left transmission zero at 11.63 GHz is from the coupling between the resonance modes at 11.82 GHz and 12.12 GHz, and these two modes are with inversed phases. Correspondingly, transmission zero near the right passband edge is from the coupling between resonance modes at 12.12 GHz and 12.33 GHz, and they share the same phases.

## 4. CONCLUSION

A monolithic three dimensional frequency selective structure with dual passbands has been put forward, and the working principles and design have been comprehensively investigated with simulations. The lower quasi-elliptic passband is comprised of two resonances, among which the first resonance roots in the front ring resonance and the second comes from TE120 cavity resonance mode. The transmission zero near the right edge of lower passband is from the coupling between slot resonance and TE120 cavity resonance. Besides, the upper elliptic passband is characterized with three resonances and two transmission zeros near each band edges, and they are proved to originate from the slot resonance modes of front rings, lateral rings as well as their mutual coupling. As to the design, the resonance frequencies of lower passband can be roughly estimated combining the operating principles and the calculating equations. The upper passband is also easy to design as the resonance frequencies are controlled almost separately by different rings. This work also proves that phase controlling and coupling can be used to reduce the designing complexity in producing several resonances.

In conclusion, this novel dual-band FSS is with superior performances in high selectivity, rapid rolloff, and high attenuation in stopband. Moreover, its working principle is clear and the design is simple. This work will help to advance the exploration of elliptic FSS and its application.

This work might be expensive to fabricate with traditional method at present, however the fabrication is believed to be easy and inexpensive in the near future with the revolutionary change brought by Three-dimensional Printing Technology.

## ACKNOWLEDGMENT

The authors would like to give special thanks to Mr. Cheng Yang for valuable discussions and suggestions in analysis.

## REFERENCES

1. Rashid, A. K. and Z. Shen, "Three-dimensional frequency selective surfaces," *Int. Conf. Communications, Circuits, and Systems (ICCCAS)*, China, Jul. 2010.
2. Lu, Z.-H., P.-G. Liu, and X.-J. Huang, "A novel three-dimensional frequency selective structure," *IEEE Antennas and Wireless Propagation Letters*, Vol. 11, 588–591, 2012.

3. Abbaspour, A., K. Sarabandi, and G. M. Rebeiz, "Antenna-filter-antenna array as a class of bandpass frequency selective surfaces," *IEEE Trans. on Microwave Theory and Tech.*, Vol. 52, No. 8, 1781–1789, 2004.
4. Luo, G. Q., W. Hong, Z. C. Hao, B. Liu, W. D. Li, J. X. Chen, H. X. Zhou, and K. Wu, "Theory and experiment of novel frequency selective surface based on substrate integrated waveguide technology," *IEEE Trans. on Antennas and Propag.*, Vol. 53, 4035–4043, 2005.
5. Zuo, Y., A. K. Rashid, Z. Shen, and Y. Feng, "Design of dual-polarized frequency selective structure with quasi-elliptic bandpass response," *IEEE Antennas and Wireless Propagation Letters*, Vol. 8, 624–626, 2012.
6. Munk, B. A., *Frequency Selective Surface: Theory and Design*, Wiley-Interscience, New York, 2011.
7. Bianchi, G. and R. Sorrentino, *Electronic Filter Simulation & Design*, McGraw-Hill, New York, 2007.
8. Luo, G. Q., W. Hong, Q. H. Lai, K. Wu, and L. L. Sun, "Design and experimental verification of compact frequency-selective surface with quasi-elliptic bandpass response," *IEEE Trans. on Microwave Theory and Tech.*, Vol. 55, 2481–2487, 2007.
9. Rashid, A. K., Z. Shen, and B. Li, "An elliptical bandpass frequency selective structure based on microstrip lines," *IEEE Trans. on Antennas and Propag.*, Vol. 60, 4661–4669, 2012.
10. Yang, H.-Y., S.-X. Gong, P.-F. Zhang, and Y. Guan, "Compound frequency selective surface with quasi-elliptic bandpass response," *Electronics Letters*, Vol. 46, No. 1, 7–8, 2010.
11. Luo, G. Q., W. Hong, H. J. Tang, J. X. Chen, and K. Wu, "Dualband frequency-selective surfaces using substrate-integrated waveguide technology," *IET Microw. Antennas Propag.*, Vol. 1, No. 2, 408–413, 2007.
12. Alan Davis, W., *Radio Frequency Circuit Design*, John Wiley & Sons, Inc., New York, 2011.
13. Harrington, R. F., *Time-harmonic Electronmagnetic Fields*, IEEE Press, John Wiley & Sons, Inc., New York, 2001.
14. Zhang, Y. and G. Liu, "Analysis of resonance frequency for rectangular cavity with apertures and embedded materials," *Proc. Int. Conf. Intelligent Computing and Intelligent Systems*, 271–273, 2010.